COMPARISON OF EXPERIMENTAL RESULTS AND NUMERICAL CALCULATIONS OF ULTRASONIC WAVES SCATTERING ON A MODEL OF THE ARTERY

JANUSZ WOJCIK, ZBIGNIEW TRAWINSKI, TADEUSZ POWALOWSKI†

Ultrasonic Department, Institute of Fundamental Technological Research, Polish Academy of Sciences
21 Swietokrzska Str., 00-049 Warsaw, Poland
jwojcik@ippt.gov.pl

The aim of this paper is to compare the results of the mathematical modeling and experimental results of the ultrasonic waves scattering in the inhomogeneous dissipative medium. The research was carried out for an artery model (a pipe made of a latex), with internal diameter of 3, 5 and 8 mm and wall thickness of 0.75, 1.25 and 2 mm. The numerical solver was created for calculation of the fields of ultrasonic beams and scattered fields under different boundary conditions, different angles and transversal displacement of ultrasonic beams with respect to the position of the arterial wall. The investigations employed the VED ultrasonic apparatus. The frequency of the transmitted ultrasound was 6.75 MHz. The good agreement between the numerical calculation and experimental results was obtained. The numerical solver is used for verified proposed methods for determining of the IMT in the artery walls.

INTRODUCTION

The pathological process of atherosclerosis development and its connection with alterations that occur in walls of blood vessels present a matter of interest for numerous scientificfic and clinical centers worldwide. In case of non-invasive investigations, the ultrasonic measurements for momentary diameters of arteries over the entire cardiac cycle serve as the basis enabling to determine elasticity of arterial walls. Maximum and minimum values for the vessel diameter are associated with respective systolic and diastolic blood pressures measured by a sphygmomanometer. Based on the above measurements, the elasticity factors of the arterial wall are determined [1,2]. In case of non-invasive ultrasonic measurement, reproducibility of the obtained results is an extremely important parameter, since it is used to define sensitivity of the diagnostic tool [3]. The major objective of the thesis was to develop a mathematical model that would be capable of describing spatial and time-

dependent distribution of an ultrasonic beam that is emitted by a piezoelectric ring transducer and then scattered on cylindrical surfaces of the walls in artery models. The developed model was tested for results of experiments when an elastic pipe was immersed in water. The investigations were carried out using the VED equipment, designed and constructed in the Ultrasonic Department of the Institute of Fundamental Technological Research of the Polish Academy of Sciences, purposefully dedicated for elasticity examination of arterial walls in human body.

1. PHYSICAL MODEL

1.1 BASIC EQUATIONS

With use of non-dimensional variables, the equation that defines the propagation of sonic waves in a homogenous (with undisturbed parameters of the material) non-linear and absorbing medium, can be expressed by the following equation [4]:

$$\Delta P - \partial_{tt} P - 2\partial_t \mathbf{A} P + q\beta\, \partial_{tt}\left(P\right)^2 = 0 \qquad (Eq.1)$$

$$\mathbf{A}P \equiv A(t) \otimes P(\mathbf{x},t),\ A(t) = F^{-1}\left[a(n)\right]$$

where: $P(\mathbf{x},t)$ is the pressure in the 3D coordinate system $\mathbf{x}$ at the moment of time t; $\mathbf{A}$ is a convolution-type operator that defines absorption; q is the Mach number (in our case the Mach number is calculated for velocities on the surface of the disturbance); $\beta \equiv (\gamma+1)/2$; $\gamma \equiv (B/A)+1$ or γ - adiabatic exponent, $n \equiv f/f_0$ - non-dimensional frequency; f , f_0 - respectively: frequency and characteristic frequency; $a(n)$ -the small signal coefficient of absorption, $\mathbf{A} = F^{-1}\left[a(n)\right]$, $F[\cdot]$ - Fourier transform.

1.2 EQUATION FOR NON-HOMOGENOUS MEDIUM

For a medium, where areas with disturbed parameters of the wave-carrying material occur (e.g. with values that differ from the ones for the entire wave propagation area or due to "inclusion" of admixtures with such material properties that are different than the ones for the surrounding medium), the equation (1) can be expressed in the following manner:

$$\Delta P - \partial_{tt} P - 2\partial_t \mathbf{A}P + q\beta\partial_{tt}(P)^2 = -\Pi\partial_{tt}P + \Gamma q\beta\partial_{tt}(P)^2$$
$$(Eq.2)$$
$$\Pi(\mathbf{x}) \equiv 1 - \frac{1}{c_r^2},\quad \Gamma(\mathbf{x}) \equiv 1 - \frac{\beta_r}{g_r c_r^4}$$

where: $c_r(\mathbf{x}) \equiv c_1(\mathbf{x})/c$, $g_r \equiv g_1/g$, $\beta_r \equiv \beta_1/\beta = (\gamma_1+1)/(\gamma+1)$. Respectively, c_1, g_1 and γ_1 stand for sound velocity, density and "adiabatic exponent" within the disturbed area. In our case, $c = 1$ denotes the non-dimensional sound velocity in the surrounding reference medium, e.g. in water. The (Eq.2) neglects perturbations $\delta\mathbf{A} \equiv \mathbf{A}_1 - \mathbf{A} = F^{-1}\left[a_1(n) - a(n)\right]$ as the algorithms that was developed by us makes it possible to achieve uniform solutions (in terms of absorption) of the model equations for all possible values of absorption and spatial configuration of absorbing constituents that have any importance for us. The Π and Γ factors may be defined as scattering potentials: linear Π and non-linear Γ .

1.3 DERIVATION OF MODEL EQUATIONS FOR THE ISSUES OF BACKSCATTERING

For derivation of defining equations for our model we made the following assumptions:
1)   The term that is proportional to Γ describes the phenomenon of non-linear backscattering and non-linear propagation in the areas where medium parameters are disturbed. For cases that are important for our considerations the following relationship is fulfilled:

$$q\Gamma/\Pi << 1 \qquad \text{(Eq.3)}$$

Therefore the last term in (Eq.2) can be neglected. The attention should be paid to the fact that coincidence of $c_r(\mathbf{x}) \cong 1$ and $g_r \cong 1$, i.e. practical absence of linear reflection cannot be excluded, especially for biological substances. Mutual relationships between phenomena of non-linear and linear reflections are discussed in [5] and [6].
2)   Generation of scanning pulses and detection of the responding backscattered field (echo) is a typical approach in ultrasonic diagnostic techniques. Consequently, the following distribution of the acoustic field can be applied:

$$P = P^{in} + P^{sc} \qquad \text{(Eq.4)}$$

where: P^{in} corresponds to the incident (scanning) field whilst P^{sc} stands for the backscattered field. The assumption is made that P^{in} fulfils of the (Eq.1).
3)   Substitution of (4) into (2) leads to the terms that depend on $P^{in} \cdot P^{sc}$, therefore determine non-linear "cross" effects, connected with mutual intersection and interference of the incident field P^{in} with the backscattered field P^{sc} either in the area with non-disturbed parameters (the last component on the left-hand side in (Eq.2)) or, analogically, in the boundary area and in the area of disturbed parameters (the last component on the right-hand side in (Eq.2)). If scanning pulses are short, the contribution of cross-section phenomena into overall propagation-related non-linear phenomena can be omitted as duration of the time interval when a non-zero value of the product $P^{in} \cdot P^{sc}$ exists is negligibly short as compared to the lifetime of the P^{in^2} field. Cumulating of non-linear effects is a characteristic feature of the phenomena described by the (Eq.1), e.g. increasing deformation of pulses waveforms leads to extension of the Fourier spectrum. Consequently the conclusion can be made that in case of very short time intervals for interactions or propagation, the non-linear phenomena can be also omitted. Last but not least, in spite of all the foregoing deliberations, the assumption can be made that a subsequent scanning pulse is emitted only is the response (echo) of the preceding one has been received.
For all the cases that have any importance for our deliberations the assumption can be made:

$$P^{in} \cdot P^{sc} = 0 \qquad \text{(Eq.5)}$$

For insignificant differences of material parameters for the surrounding medium and the target, pressure in the backscattered field is much lower than the pressure of incident pulses $P^{sc} << P^{in}$. Hence the assumption that non-linear phenomena can be neglected for propagation of backscattered fields is absolutely justified. It must be mentioned that even those the probes that are used for ultrasonography and specified as broadband are actually of the narrow-band type, as compared to the requirements related to non-linear propagation of scanning ad

backscattered pulses. Notwithstanding the fact that propagation of backscattered signal can be really non-linear, no phenomenon related to such non-linear propagation is detected. Therefore we can assume that in the (Eq.2)

$$qP^{sc^2} = 0 \qquad \text{(Eq.6)}$$

After having taken into account the foregoing assumptions from the (Eq.2), the following formula can be obtained to define backscattered fields.

$$\Delta P^{sc} - \partial_{tt} P^{sc} - 2\partial_t \mathbf{A} P^{sc} = -\Pi \partial_{tt} (P^{sc} + P^{in}) \qquad \text{(Eq.7)}$$

where the incident field P^{in} fulfils the equation:

$$\Delta P^{in} - \partial_{tt} P^{in} - 2\partial_t \mathbf{A} P^{in} + q\beta \partial_{tt} (P^{in})^2 = 0 \qquad \text{(Eq.8)}$$

The only non-linear equation is the one numbered as (8) and it determines propagation of scanning pulses. However, if the excitation level is low, still that equation can be linearized as well by omitting the last component. Equations (Eq.7) and (Eq.8) represent our mathematical model for physical phenomena that take place in the areas of propagation and scattering of ultrasonic signals.

2. SOLVER

Construction of a solver for scattered fields is the fundamental issue for setting up a numerical model of an experiment that is aimed to reflect real situations that occur in ultrasonography practice. The solver that we constructed for our own needs is composed of three parts: 1)Solver for the incident field. It is the solver that bases on codes JWNUT2D and JWNUT3D, which we have been using for many years. The first code solves the (Eq.8) in the axially symmetrical cases, the second one is applicable to whichever one-sided boundary conditions (see [7]); 2)Solver for the scattered field. It is the tool that is able to calculate parameters of backs-scattered fields and their pressures on the detector surface, whereas the tool uses numerically determined incident field and information on geometrical and material parameters of the target as the basis for calculations; 3)Simulator of electronic tracks that is used for calculation of pulse responds $h(t)$ to electronic tracks. Distribution of pressure on the surface of the probe is averaged over the entire head surface (the theory of piezoelectric phenomena says that electric signals at head output are proportional to the aforementioned average value).

$$P_E(t) = \frac{1}{S} \int_{S(\mathbf{x})} P^{sc}(S(\mathbf{x}), t) Ap(S(\mathbf{x})) dS \qquad \text{(Eq.9)}$$

where $S(\mathbf{x})$ denotes a point on the transducer surface, S stands for the transducer surface area and $Ap(S(\mathbf{x}))$ is the apodization function for the transducer surface. In this study $P_E(t)$ is referred to as the echo. The RF signal $P_{RF}(t)$ represents a single line of scanning and is calculated as follows:

$$P_{RF}(t) = h(t) \otimes P_E(t) \ , \ h = \mathrm{F}^{-1}[H(n)] \qquad \text{(Eq.10)}$$

where $H(n)$ is the system transmittance.

3. RESULTS

Experimental setup is shown on Figure 1. The research was carried out for a pipe made of latex, with internal diameter of 5 mm and wall thickness of 1.25 mm. The ultrasonic beam was focused in water medium, at the depth of 23 mm from the transducer surface. Transducer diameter was 6 mm. The investigations employed the VED ultrasonic apparatus. The frequency of the transmitted ultrasound was 6.75 MHz. The pulses were measured by means of the hydrophone of the type: Sonic Technologies Model 800 Bilaminar Hydrophone. During the performed research the front surface of the pipe wall was positioned in the focus of the ultrasonic probe. The RF electric signal, $P_{RF}(t)$, corresponding to echoes reflected by the pipe walls, was recorded at the output of the RF receiver by means of the digital oscilloscope AGILENT 54641D. To highlight relationships between target (pipe) dimensions and wavelength of the echoed signals (both acoustic waves and corresponding electric waveforms) the scales were converted all the time into 3D ones and expressed in millimeters. Spatial size of the measurement "window" was 30 mm. Signal amplitudes were presented as relative values. Results for calculations and measurements are presented in Figures 2 - 7.
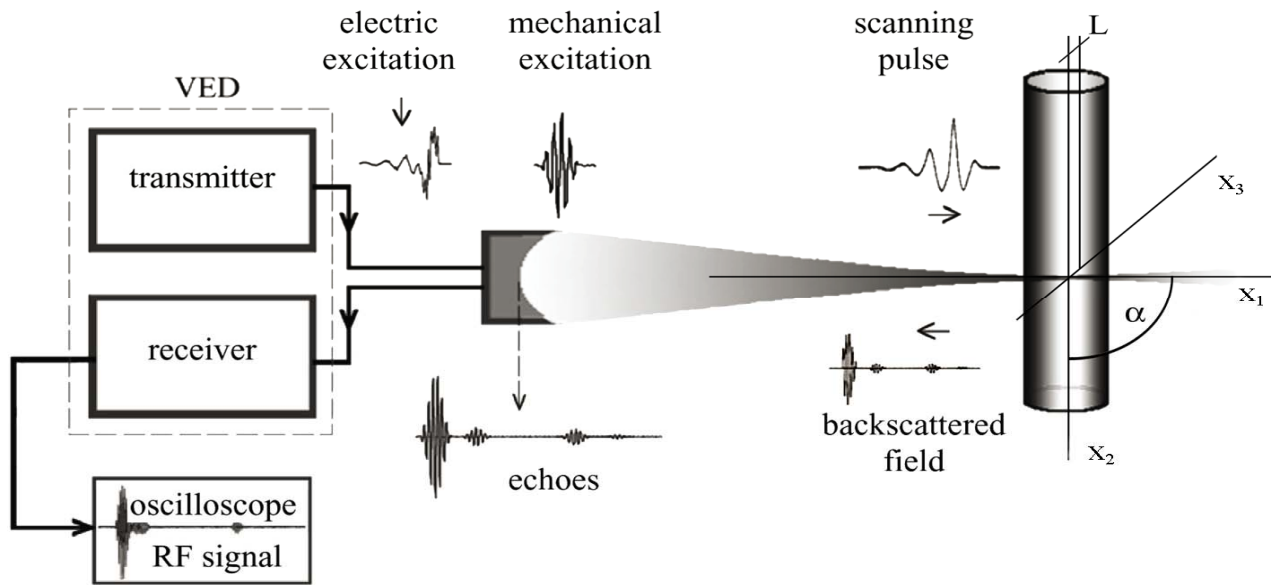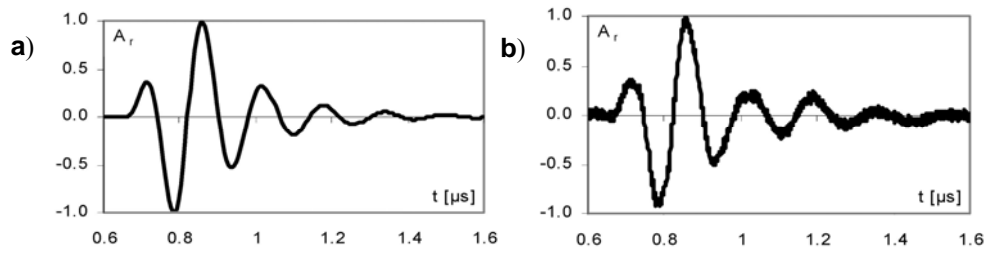

Fig.1 Experimental setup

Fig.2 The assumed normalized mechanical stimulation (a); the measured normalized mechanical stimulation (b), $A_r = P/P_0$ – the relative pressure, $P_0 = 0.25$ MPa
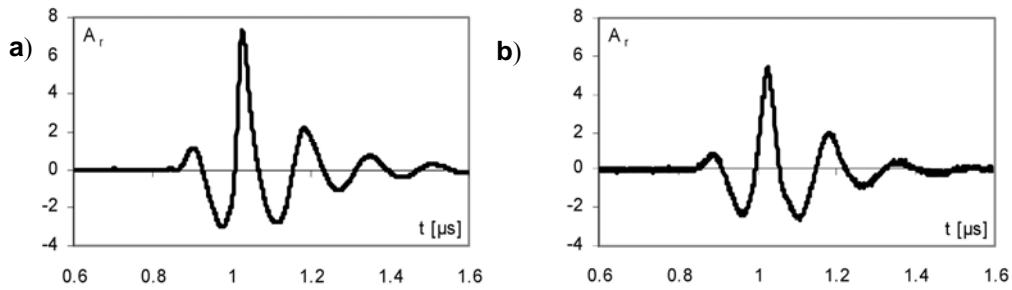

Fig.3 The normalized scanning pulse in the focus (a) calculated from the numerical model by means of the formula (8); the normalized scanning pulse measured in the focus (b). A_r - the relative pressure
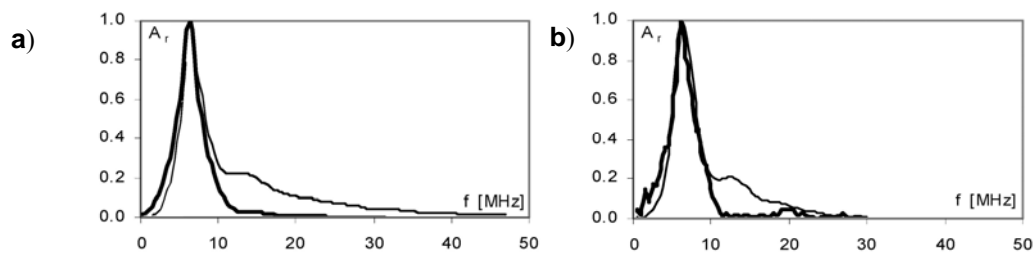

Fig.4 a) the normalized spectrum of the assumed mechanical stimulation (thick line) and the normalized spectrum of the calculated scanning pulse in the focus (thin line); b) the normalized spectrum of the measured mechanical stimulation (thick line) and the normalized spectrum of the measured scanning pulse in the focus (thin line), A_r –the relative amplitude
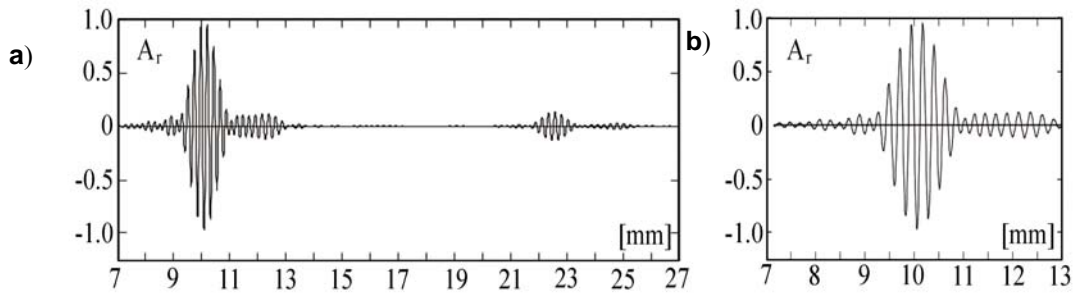
Fig.5 a) The RF signal $P_{RF}(t)$ calculated from the numerical model by means of the formula 2; b) the expanded RF signal, from the first pipe wall. Ar - the relative amplitude (with respect to the maximum value of the RF signal amplitude)
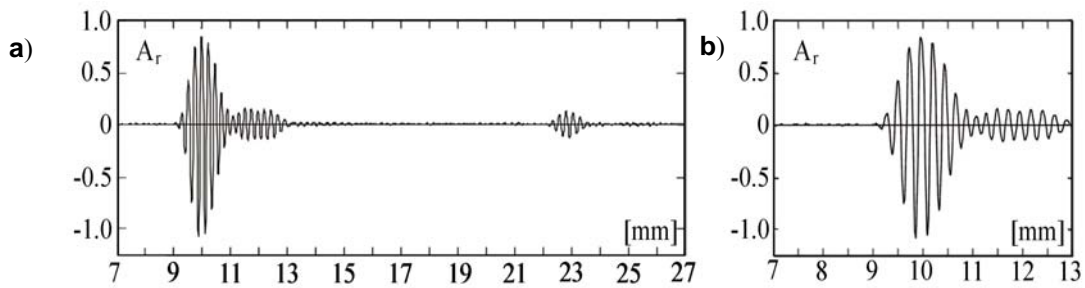

Fig.6 a) The RF signal $P_{RF}(t)$ measured by means of the VED apparatus; b) the expanded RF signal from the proximal pipe wall, Ar - the relative amplitude (with respect to the maximum value of the RF signal amplitude)
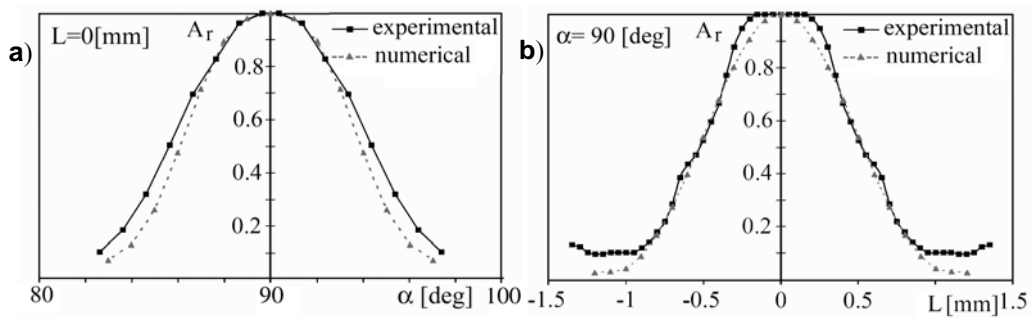

Fig.7 a) Changes of the maximal RF-signal amplitude as a function of angle α and - b) the transversal displacement L of the ultrasonic beam axis x_1, with respect to the arterial model axis x_2 (see Figure 1) for phantom diameter 5mm. A_r - maximal RF-signal amplitude with respect to the maximal RF - signal amplitude for the angle α = 90 deg and transversal displacement L = 0mm
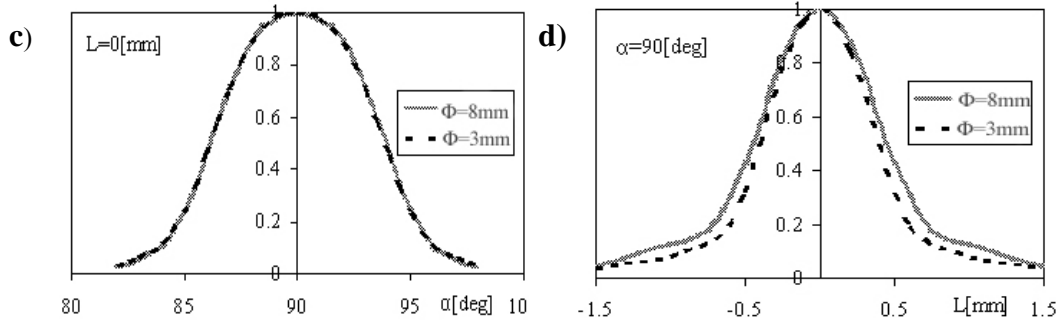
Fig.8 Results of calculations for phantom diameter 8mm and 3mm. -c) for the transversal displacement L = 0mm. - d) for the angle a = 90deg. A_r - maximal RF-signal amplitude with respect to the maximal RF – signal amplitude

4. SOLVER APPLICATION

4.1 IMT EXAMINATION

The examination of the change in the artery wall thickness was carried out by solver on a numerical model. The artery wall is composed of three layers: the adventitia, the media and the intima. The wall thickness changed under the blood pressure change during the cardiac cycle. The intima-media thickness (IMT) was calculated on the basis of the distance between two successive echoes which correspond to reflection from intima and adventitia layers respectively for the given IMT1 -intima+media thickness in the numerical model. The zeros crossing [] and the correlation methods was used for IMT_{ZC} and IMT_{COR} determination.

The internal radius of the artery numerical model was 3 mm for the diastolic pressure and 3.3 mm for the systolic pressure. For diastolic pressure, the thickness of the intima, the media and the adventitia layer was equal to 0.12 mm, 0.36 mm and 0.12 mm respectively. Taking into account the incompressibility of the material, from which the artery wall was made, the IMT1 was changed from 0.48 mm to 0.44 mm respectively [9].

4.2 METHODS EXAMINATION

For the ideal method of the IMT determination the relation between truth end estimated value is as follows:

$$IMT (IMT1) = a \cdot MT1 + b$$

(Eq.11)
where: $a = 1$, $b = 0$.
In our numerical experiment we obtained:

$$IMT_{ZC} = 0.8306 \cdot MT1 + 0.1254 \qquad (Eq.12)$$

$$IMT_{COR} = 1.2469 \cdot MT1 - 0.0712 \qquad (Eq.13)$$

That means, that the zero-crossing method is under- ($a<1$), during the correlation method is over - estimated ($a>1$) (see Figure 9).
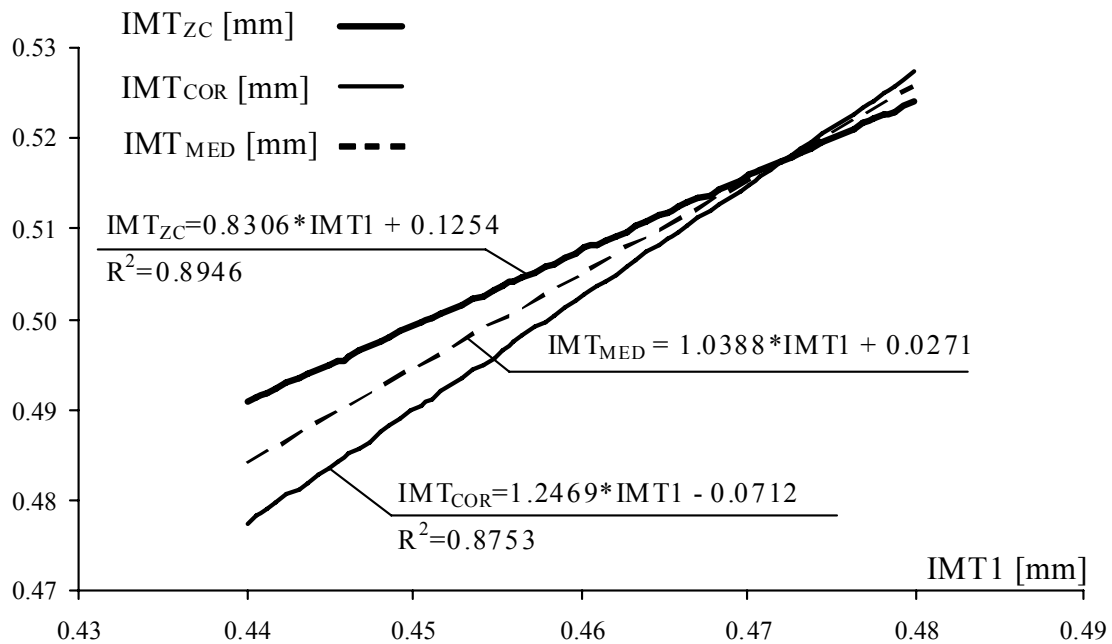
Fig.9 Numerical experiment. Comparison of the methods used for IMT examination.
IMT1-thrue values. IMT_{ZC}- results obtained on the base of the zero-crossing method
IMT_{COR}- results obtained on the base of the correlation method.
IMT_{MED}- mean values – dashed line

The $IMT_{MED} \equiv (IMT_{ZC}+IMT_{COR})/2$ denotes averaging results obtained from both methods. As we see for IMT_{MED} $a=1.0388 \approx 1$; $b=0.0271$. That confirms our hypothesis that combination of the both methods gives results very closed to the ideal (see Figure 9).

5. CONCLUSIONS

Comparison between the results that were obtained from numerical calculations and from measurements (Figures. 2 – 7) serves as a proof that the numerical model that was developed by our own enables simulation of the experiments with a good coherence. It is the matter of high importance when the designing process of measurement equipment is to be optimized. More expanded discussion see [8]. Results obtained on the basis of numerical calculations in the controlled environment (IMT1) permitted for determining the zero-crossing method and the correlated method as under estimated and over estimated methods respectively, hence, the results obtained after averaged results from both methods involve a very small error of the estimation, relatively lowest, compare to the each of them (see Figure 9).

REFERENCES

1. T. Powalowski, Z. Trawinski, L. Hilgertner, Archives of Acoustics 28, 325–337, (2003).
2. T. Kawasaki, S. Sasayama, S. YagI, T. Asakawa, T. Hirai, Non-invasive assessment of the

Age related changes in stiffness of major branches of the human arteries. Cardiovascular Research 21**,** 678–687, (1987).

3. T. Szymonski, M. Lapinski, T. Powalowski, Z. Trawinski, Evaluation of the reproducibility of vascular echo doppler system for the assessment of the carotid artery elasticity. Acta Angiologica 3, 83–91, (1997).

4. J. Wojcik, Conservation of energy and absorption in acoustic fields for linear and nonlinear propagation. J. Acoust. Soc. Am. 104**,** 2654–2663, (1998).

5. J. Wojcik, Nonlinear reflection and transmission of plane acoustics waves. Archives of Acoustics 29, 607–632, (2004).

6. A. Nowicki, J. Wójcik, W. Secomski, Harmonic Imaging Using Multitone Nonlinear Coding. Ultrasound in Medicine and Biology (2007).

7. J. Wojcik, A. Nowicki, P.A. Lewin, P.E. Bloomfield, T. Kujawska, L. Filipczynski†, Wave Envelopes Method for Description of Nonlinear Acoustic Wave Propagation. Ultrasonics 44, 310–329, (2006).

8. J.Wojcik, T. Powalowski, R. Tymkiewicz, A. Lamers, Z. Trawinski, Scattering of ultrasonic wave on a model of the artery. Archives of Acoustics 31. 4, 471–479,(2006).

9. T. Powalowski, J. Wojcik, Z. Trawinski, Numerical solver of acoustic field in simulation of artery wall thickness examinations. Hydroacoustics Vol.10. 163-168, (2007).